Liquid Crystals
Publication details, including instructions for authors and subscription information:
http://www.informaworld.com/smpp/title~content=t713926090

Lehmann effect in chiral liquid crystals and Langmuir monolayers: an experimental survey

P. Oswald[a]; A. Dequidt[a]
[a] Université de Lyon, Ecole Normale Supérieure de Lyon, Laboratoire de Physique, Lyon, France

First published on: 29 June 2009

To cite this Article Oswald, P. and Dequidt, A.(2009) 'Lehmann effect in chiral liquid crystals and Langmuir monolayers: an experimental survey', Liquid Crystals, 36: 10, 1071 — 1084, First published on: 29 June 2009 (iFirst)
To link to this Article: DOI: 10.1080/02678290902775281
URL: http://dx.doi.org/10.1080/02678290902775281

Liquid Crystals,
Vol. 36, Nos. 10–11, October–November 2009, 1071–1084

Taylor & Francis
Taylor & Francis Group

INVITED ARTICLE

Lehmann effect in chiral liquid crystals and Langmuir monolayers: an experimental survey

P. Oswald* and A. Dequidt

Université de Lyon, Ecole Normale Supérieure de Lyon, Laboratoire de Physique, 46 Allée d'Italie, 69364 Lyon, France

(Received 22 November 2008; final form 19 January 2009)

In 1900 Otto Lehmann observed that the internal texture of cholesteric droplets, when submitted to a thermal gradient, was constantly rotating. This phenomenon was explained phenomenologically in 1968 from symmetry arguments by F.M. Leslie in the framework of the nematodynamics. Six years later, Pierre-Gilles de Gennes noted in a premonitory way, in his seminal book *The Physics of Liquid Crystals*, that the heat current responsible for the Lehmann effect could also be an electric or a diffusion current, suggesting the existence of an electric or chemical Lehmann effect. This led to numerous experiments, sometimes wrongly interpreted, and to the recent discovery of the chemical Lehmann effect in Langmuir monolayer and ferroelectric smectic films. These experiments are reviewed and discussed in this paper.

Keywords: Lehmann effect (thermal, electric and chemical); flexoelectricity; cholestric finger; spiral; Langmuir monolayer

1. Introduction

In his pioneer work of 1900 (*1*), Lehmann was working with a cholesteric liquid crystal. This mesophase, the structure of which was elucidated in 1925 by Friedel (*2*), is a twisted nematic phase composed of optically active molecules. We recall that in the nematic phase the rod-like molecules align along a single direction characterized by a unit vector: the director $\boldsymbol{n}$ (with $\boldsymbol{n} \Leftrightarrow -\boldsymbol{n}$). In the cholesteric phase, the director rotates at equilibrium around a space direction called the helical axis (Figure 1). Note that the symmetry group of the nematic phase is $D_{\infty h}$ whereas that of the cholesteric phase is D_2.

In the work of Lehmann, the cholesteric phase was obtained by dissolving a small quantity of a chiral substance (colophane or cholesteryl benzoate) in the nematic liquid crystal para-azoxyphenetol. Lehmann observed that droplets of the cholesteric phase in coexistence with the isotropic liquid were rotating when heated from below. As the para-azoxyphenetol melts at high temperature, around 130°C, one can expect that the Lehmann samples were subjected to pretty large temperature gradients.

Some drawings by Lehmann of the droplets are shown in Figure 2. Each droplet presents a characteristic spiraling texture which rotates at constant velocity under the action of the temperature gradient. The main observations of Lehmann are as follows.

(1) The twist and the angular velocity of the droplets simultaneously increase when the concentration of the added chiral substance is increased.
(2) The sense of rotation depends on the chiral molecule chosen, being clockwise with the colophane and anticlockwise with the cholesteryl benzoate.
(3) The rotation stops when the two chiral impurities are added in such a way that their effect on the twist of the texture disappears.

Lehmann published more detailed observations of this phenomenon in his book of 1921 (*3*). His main new observation was that it is not the droplets themselves, but just their textures inside that are rotating since no hydrodynamic motion is visible inside.

These results were qualitatively explained by Leslie in 1968 in the framework of the nematodynamics. According to Leslie (*4*), the absence of mirror and inversion symmetry in a cholesteric phase allows a coupling between the temperature gradient ∇T and the director $\boldsymbol{n}$, resulting in a bulk torque of expression:

$$\boldsymbol{\Gamma}_{\mathrm{Leh}} = -\nu \boldsymbol{G}_{\perp} \tag{1}$$

where $\boldsymbol{G}_{\perp} = (\boldsymbol{n} \times \nabla) \times \boldsymbol{n}$ is the component of the temperature gradient perpendicular to $\boldsymbol{n}$. The phenomenological coefficient ν is now called the Lehmann coefficient.

Present address: Laboratoire des Polymères et Matériaux Avancés Centre de Recherche et de Technologie de Lyon–Rhodia, 85 rue des frères Perret, BP 62, 69192 St-FONS, France.
*Corresponding author. Email: patrick.oswald@ens-lyon.fr

ISSN 0267-8292 print/ISSN 1366-5855 online

DOI: 10.1080/02678290902775281
http://www.informaworld.com

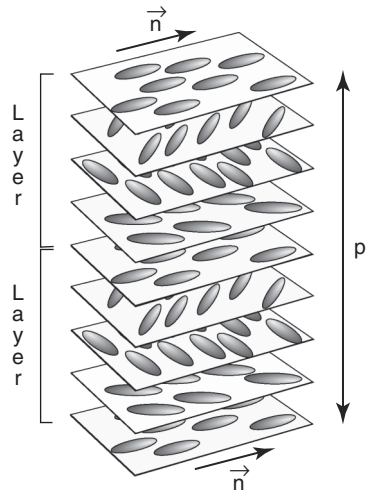

Figure 1. Structure of a cholesteric liquid crystal phase. The drawn planes are fictitious as there is no positional order in a cholesteric phase. The pitch p is the distance over which the director rotates by 2π. The true periodicity, corresponding to a 'cholesteric layer', is $p/2$ as $\boldsymbol{n}$ and $-\boldsymbol{n}$ are equivalent.

Figure 2. Drawings by Lehmann of typical cholesteric droplets continuously rotating anticlockwise when heated below (reproduced with permission from (*1*)).

Leslie's theory was then generalized by de Gennes who pointed out in his book on liquid crystals (*5*) that the heat current could also be an electric current or a diffusion current. This crucial remark opened the way to numerous experiments about the electric and more recently the chemical Lehmann effect.

The goal of this paper is to describe the main experiments performed so far in this field. For convenience, we discuss separately the three cases discussed before, without regard to the chronological order in which these experiments were performed. The plan of the article is thus very simple, the next three sections being devoted to the thermal, electric and chemical Lehmann effects, respectively, while conclusions and perspectives are drawn in the last section.

2. The thermal Lehmann effect

In this section, we describe four experiments performed in a cholesteric liquid crystal. The first was proposed by Éber and Jánossy in 1982 (*6*). This experiment was conceptually important as it showed for the first time that the Lehmann torque was measurable and not zero at the compensation temperature of a cholesteric phase. The three other experiments were performed by us in the last 2 years. The first deals with the direct experimental evidence of the continuous Lehmann rotation of the cholesteric helix in samples treated for planar and sliding anchoring. The second deals with the formation of spiraling cholesteric fingers (CF) in homeotropic samples. Finally, the last experiment is similar to that of Lehmann as it shows the rotation of cholesteric droplets at the transition temperature to the isotropic liquid.

2.1 *The Éber and Jánossy experiment*

In this experiment, a compensated cholesteric phase is sandwiched between two parallel glass plates treated for homeotropic anchoring (*6–8*). We recall that in such a cholesteric the equilibrium twist $q = -\boldsymbol{n} \cdot \nabla \times \boldsymbol{n} = 2\pi/p$ of the phase vanishes and changes sign at the compensation temperature T_c (Figure 3).

This sample is then placed into a temperature gradient parallel to the glass plates (and, thus, perpendicular to the director). In the temperature gradient, the cholesteric pitch depends on the position in such a way that a nematic homeotropic band forms between two regions filled with CF (Figure 4). We recall that CF form when the pitch is typically smaller than the sample thickness (*9, 10*).

The experiment consists of measuring very precisely the sample birefringence at the compensation temperature, i.e. in the middle of the homeotropic nematic band. Indeed, according to Leslie the director experiences a torque given by (1) to which adds another thermoelastic torque proportional to $GK_2(dq/dT)$,

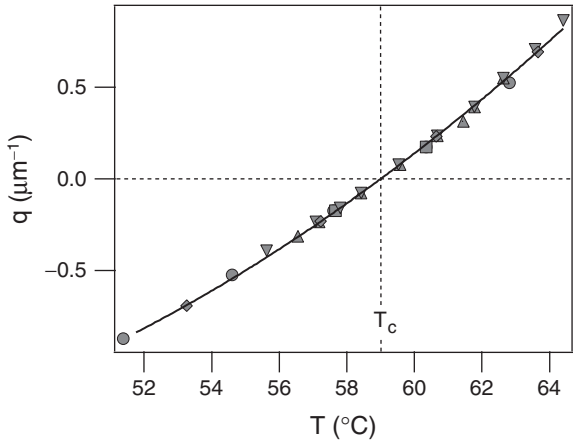

Figure 3. Equilibrium twist of a compensated cholesteric as a function of temperature. Mixture of octyloxycyanobyphenyl (8OCB) and cholesteryl chloride (CC) in mass proportion 1:1 (reproduced with permission from (*13*)).

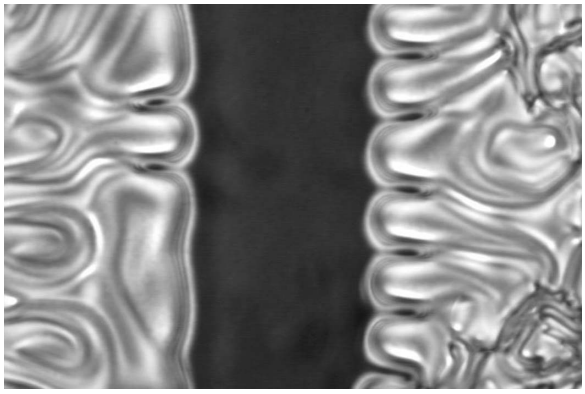

Figure 4. Homeotropic sample of a compensated cholesteric in a temperature gradient. A nematic band (black between crossed polarizers) forms between two regions filled with CF (reproduced with permission from (*14*)).

with K_2 the twist elastic constant and G the temperature gradient. These two torques make the director slightly tilt in the middle of the sample in a vertical plane orthogonal to the temperature gradient, whence a birefringence variation. This experiment allowed Éber and Jánossy to measure the effective coefficient

$$\nu_{\text{eff}} = \nu + K_2 \frac{dq}{dT}. \tag{2}$$

These authors also measured the corrective term $K_2(dq/dT)$ and finally found that the Lehmann coefficient was not zero at the compensation temperature, being of the order of 2×10^{-12} kg K^{-1} s^{-2}.

This result was important because it was the first quantitative estimate of the Lehmann coefficient in a cholesteric phase. On the other hand, it led to a polemic opposing experimentalists to theorists, the latter claiming that the Lehmann coefficient should be proportional to q (see (*11, 12*), and thus should be equal to zero at T_c.

For this reason, we repeated the experiment recently in homeotropic and also planar samples, and found again that the Lehmann coefficient was not zero at the compensation temperature (*13, 14*). More precisely, we found that in the mixture 80CB-CC (see Figure 3)

$$\nu = (2.8 \pm 0.6) \times 10^{-7}\,\text{kg}\,\text{K}^{-1}\,\text{s}^{-2}$$

at the compensation temperature. This value is very close to that given by Éber and Jánossy in a similar mixture (8CB + CC in mass proportion 1:1).

This result led us to reconsider the arguments of theorists about this problem and to realize that the symmetry group of a compensated cholesteric is different from that of an usual nematic. Indeed, a compensated cholesteric has no mirror or inversion symmetry in spite of its nematic-like structure (its helix is unwound) because it is composed of chiral molecules. For this reason, its symmetry group is D_∞ and differs from that $D_{\infty h}$ of a usual nematic made of non-chiral molecules, a point that theorists did not realize at the time (*12*).

As a consequence, the Lehmann coefficient has no reason to vanish at the compensation temperature, in agreement with experiments. The two experiments presented in the following two sections confirm this point.

2.2 Direct experimental evidence of the helix rotation in planar samples

It turns out that the previous experiment is static and delicate as it does not directly show the continuous Lehmann rotation. Indeed, the director cannot freely rotate in this experiment because it is strongly anchored to the cell surfaces.

For this reason, we performed the basic experiment described by de Gennes in his book (*5*). In this experiment (*15*), the cholesteric is confined between two parallel glass plates treated for planar and sliding anchoring. For this purpose a new surface treatment was used, which is described in (*16*). The sample is then sandwiched between two transparent ovens which impose a controlled temperature gradient. In this geometry, the helix axis is perpendicular to the glass plates and parallel to the temperature gradient. As a consequence, it experiences a constant Lehmann torque of amplitude $-\nu G$ which equilibrates with the viscous torque of amplitude $\gamma_1\omega$. The resulting angular velocity ω of the helix thus simply reads (*5*):

$$\omega = -\frac{\nu G}{\gamma_1}, \tag{3}$$

where γ_1 is the bulk rotational viscosity. In practice, this formula is incomplete because it does not take into account the viscous dissipation at the surfaces. Doing this leads to replacing γ_1 by the effective viscosity $\gamma_1^* = \gamma_1 + 2\gamma_S/d$ in the previous formula, where γ_S is a phenomenological rotational surface viscosity and d the sample thickness (*15*).

In order to measure ω, a planar sample of the compensated mixture 80CB + CC (see Figure 3) was prepared. As the anchoring is sliding, it is also degenerate which allows the director to form disclination lines. These defects can be easily seen under the microscope between crossed polarizers. Almost all of them are $\pm 1/2$ disclination lines, the sign of which can be easily found by rotating the polarizers. Figure 5 shows

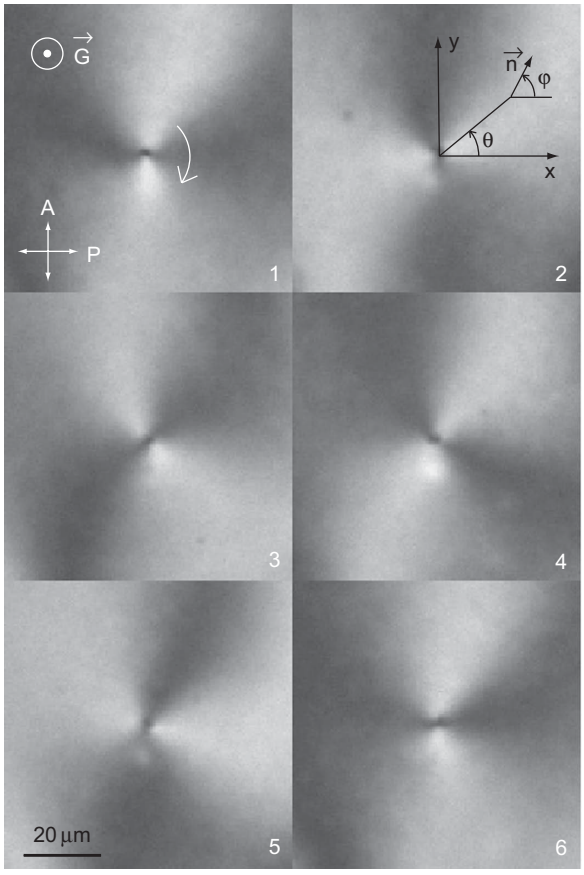

Figure 5. The two extinction branches of a −1/2 disclination rotate clockwise when the temperature gradient points upwards. The time interval between two photographs is 11 s. Here $T = T_c$, $d = 25\ \mu$m and $G \approx 6 \times 10^4$ K m^{-1} (reproduced with permission from (*15*)).

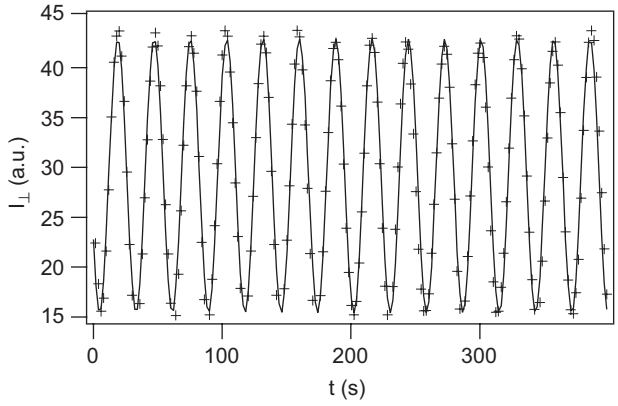

Figure 6. Intensity measured at one point of the sample between crossed polarizers as a function of time. The solid line is a fit to a sine function of angular frequency 4 ω. Here $T = T_c$, $d = 25\ \mu$m and $G \approx 6 \times 10^4$ K m^{-1} (reproduced with permission from (*15*)).

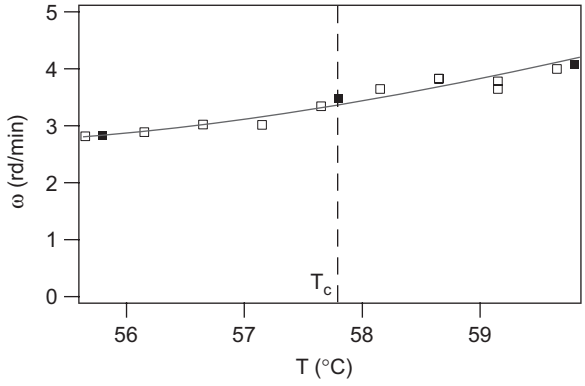

Figure 7. Angular velocity as a function of the sample temperature. $d = 25\ \mu$m and $G \approx -6 \times 10^4$ K m^{-1}. Note that $\omega > 0$ when $G < 0$ which shows that $\nu > 0$ at all temperatures according to (3) (reproduced with permission from (*15*)).

a −1/2 line. The experiment shows that when a temperature gradient is imposed on the sample, the two extinction branches start to rotate because of the local rotation of the cholesteric helix described above. This rotation is very regular as can be seen from the recording of the transmitted intensity displayed in Figure 6. In addition, it can be easily checked that the sense of rotation of the extinction branches of the disclination depends on the sign of the Lehmann coefficient for a given temperature gradient. This experiment thus allowed us to measure the ratio ν/γ_1^*, as well as the sign of the Lehmann coefficient as a function of temperature, directly. We found that the Lehmann coefficient is positive in the 80CB-CC mixture at all temperatures and does not vanish at T_c (Figure 7). In addition, we measured the viscosities γ_1 and γ_S at the compensation temperature ($\gamma_1 \approx 0.075$ Pa s and $\gamma_S \approx 3 \times 10^{-7}$ Pa s m, see (*16*)), which allowed us to finally estimate the Lehmann coefficient at this temperature:

$$\nu \approx 1 \times 10^{-7}\ \mathrm{kg\,K^{-1}\,s^{-2}}.$$

This value is smaller than that found from the static method (see the previous section), but of the same order of magnitude. The reason of this discrepancy is unclear, but could come from some underestimate of the surface viscosity.

2.3 Thermomechanically driven drift of CF in homeotropic samples

In 1997, Gil and Thiberge (*17*) showed theoretically that CF must drift perpendicularly to their axes when they are subjected to a Lehmann torque. In their calculation they assumed that the torque was due a DC electric field, but the same calculation also applies for a temperature gradient. For this reason,

we performed the experiment in a temperature gradient with the same compensated mixture as before (Figure 3) (*18*). Samples were homeotropically oriented which is the condition to form CF. Different types of CF exist with different director field topologies. In this experiment, we only worked with CF1 (Figure 8), i.e. with CF of the first type which are continuous everywhere (other fingers contain singularities).

These fingers form and coexist with the nematic homeotropic phase (i.e. the unwound cholesteric) when the cholesteric pitch is of the order of the sample thickness (*9*, *10*). To fulfill this condition, it is thus necessary to adjust the temperature of the sample carefully when it is placed in a temperature gradient. This temperature obviously depends on the sample thickness chosen, since the pitch rapidly changes with the temperature around T_c (Figure 3).

Let us now consider a sample of a given thickness in the temperature gradient. After adjusting its temperature, we observed the nucleation and growth of CF. Most of them nucleate on dust particles from which they grow. We observed that, during the growth, the fingers drift perpendicularly to their axes and form spirals rotating at a constant angular velocity. A nice example of a triple spiral with its centre pinned on a dust particle is shown in Figure 9. Single spirals can also form with two free ends. Two such spirals observed in the same sample below and above T_c and under the same temperature gradient are shown in Figure 10. The crucial point here is that the two spirals *rotate in the same direction* in spite of the change of sign of the equilibrium twist. It can be shown (*18*) from this observation and the theoretical model that the Lehmann coefficient does not change sign at T_c and is always positive. In addition, the Lehmann coefficient can be estimated as a function

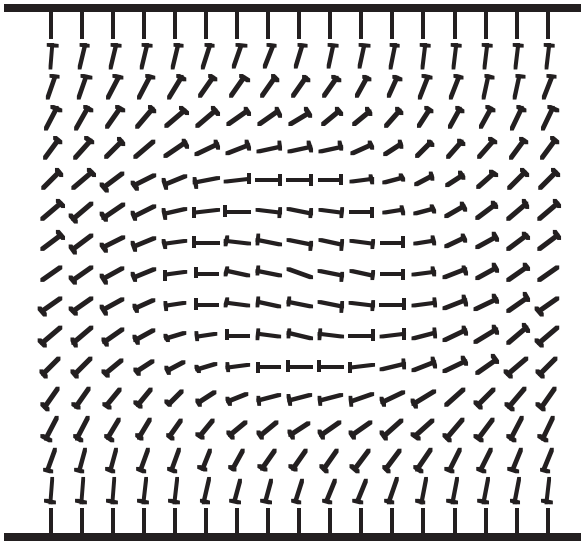

Figure 8. Nail representation of the director field inside a CF1. Section perpendicular to the finger axis (reproduced with permission from (*15*)).

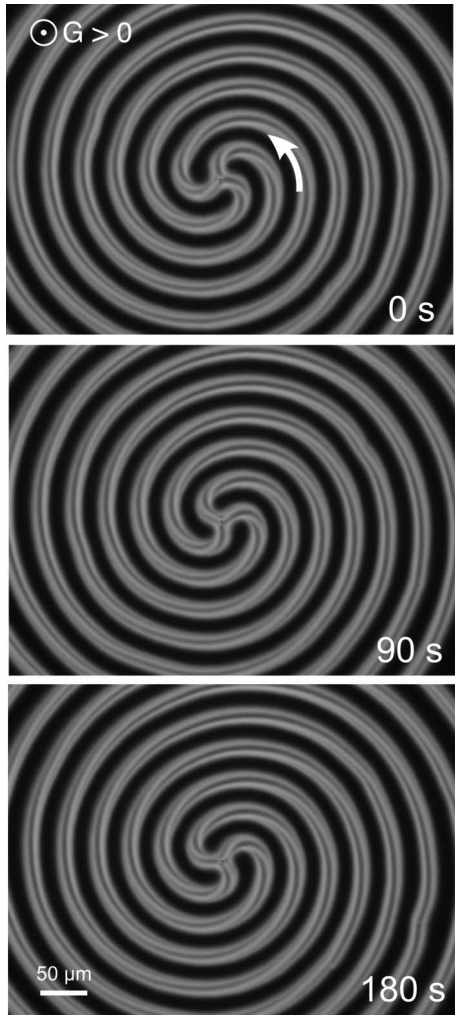

Figure 9. Triple spirals rotating anticlockwise under the action of a temperature gradient pointing upwards. Here $T = T_c + 3.3°C$, $d = 10\ \mu m$ and $G \approx 5 \times 10^4$ K m^{-1} (reproduced with permission from (*18*)).

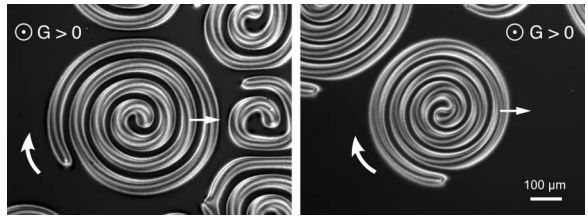

Figure 10. Two single spirals rotating in the same direction in a 25 μm-thick sample above and below T_c: (a) $T = T_c + 1.4°C$; (b) $T = T_c - 1.1°C$. In both cases $G \approx 7 \times 10^4$ K m^{-1} (reproduced with permission from (*18*)).

of temperature on both sides of T_c by comparing the finger drift velocity to its theoretical expression

$$V = A\frac{\nu G d}{\gamma_1}, \tag{4}$$

where A is a dimensionless factor which only depends on the finger topology ($A \approx 0.14$, see (*17*)).

From these measurements, we obtained after extrapolation to T_c that

$$\nu \approx 2 \times 10^{-7}\,\mathrm{kg\,K^{-1}\,s^{-2}}.$$

This new value is in agreement with the two values given above.

The conclusion which thus imposes after these three experiments is that the Lehmann coefficient does not vanish at T_c in a compensated cholesteric, when it is completely unwound.

In the next section, we show that it was also possible to reproduce the original Lehmann experiment.

2.4 *Rotating droplets in planar samples*

To succeed in this experiment, we again used the cholesteric mixture 80CB + CC in mass concentration 1:1. The samples were prepared between two parallel glass plates treated for planar sliding anchoring according to the process described in (*16*). They were then placed between two transparent ovens imposing the vertical temperature gradient. The samples' temperature was adjusted in order that the cholesteric germs coexist with the isotropic liquid. Under this condition, we observed that the germs are all identical, with a banded texture inside (Figure 11(a)). More importantly, all of the droplets rotate in the same direction. Systematic measurements showed that their period of rotation increases in a quadratic way with their diameter and is inversely proportional to the temperature gradient. As a consequence, the droplets stop rotating when the temperature gradient is equal to zero and rotate in the opposite direction when the temperature gradient is reversed. We also observed that the droplets partially wet the colder plate but do not touch the other plate.

This phenomenon is very similar to the original Lehmann effect even if the texture of the droplets is different in both cases (see Figures 2 and 11 for comparison). This is certainly due to differences in the boundary conditions which are unknown in the Lehmann's work.

In order to explain our observations we developed a model in which we assumed that the director was only rotating in place under the action of the Lehmann torque. This model, which neglects all backflow

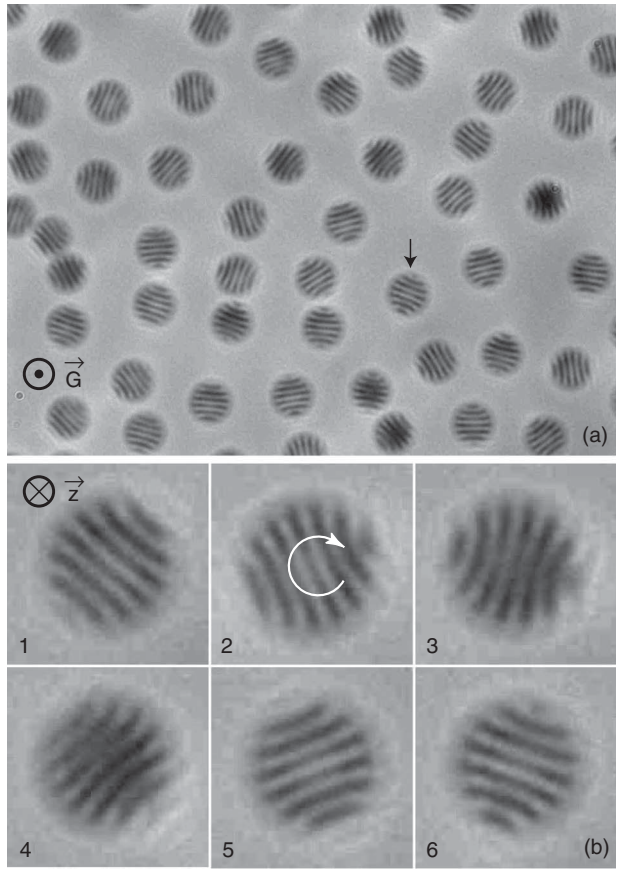

Figure 11. (a) Droplets observed in natural light. (b) Sequence of pictures showing the rotation of the droplets marked by an arrow in (a). For this temperature gradient ($G \approx -10^4$ K cm^{-1}) all droplets rotate clockwise (so that $\omega > 0$). Note that the vertical z-axis is directed downwards (reproduced with permission from (*19*)).

effects, led to the following formula for the angular frequency ω of the droplets:

$$-\frac{\nu G}{\gamma_1 \omega} = 1 + \frac{1}{16}k^2\varepsilon^2 D^2. \tag{5}$$

Here D is the droplet diameter, k is the wavelength of the banded texture and ε is the amplitude of variation of the director tilt angle in the middle of the droplet (for more details, see (*19*)). It is important to note that experimentally G and ω are of opposite signs (see Figure 11) so that the Lehmann coefficient is still positive at the melting temperature. Fitting experimental data with this equation gives the ratio

$$\frac{\nu}{\gamma_1} \approx 3.7 \times 10^{-6}\,\mathrm{m\,s^{-1}\,K^{-1}}.$$

As we were not able to measure γ_1 at the melting temperature, we performed another experiment giving

the Lehmann coefficient directly. It consisted of imposing an electric field parallel to the glass plates. The experiment showed that above some critical field E_c, all droplets stop rotating, the electric torque (proportional to $\varepsilon_0\varepsilon_a E_c{}^2$, with ε_a the dielectric anisotropy) equilibrating the Lehmann torque (proportional to νG). A straightforward calculation yields

$$\nu = f\frac{\varepsilon_0\varepsilon_a E_c^2}{2G}, \tag{6}$$

where f is a dimensionless factor which depends only on the geometry of the director field inside the droplet (to first order in ε, $f = 1$). Experimentally it was found that $E_c \approx 7 \times 10^4$ V m^{-1} for $G \approx 5 \times 10^4$ K m^{-1}. Taking $\varepsilon_a \approx 3.5$ and $f = 1$, we finally calculate that at the transition temperature,

$$\nu \approx 1.5 \times 10^{-6}\,\mathrm{kg\,K^{-1}\,s^{-2}} \quad \text{and} \quad \gamma_1 \approx 0.015\,\mathrm{Pa\,s}.$$

These results show that the viscosity decreases by a factor of five with respect to its value found at T_c (which is about 6 °C below the melting temperature), whereas the Lehmann coefficient increases by almost one order of magnitude in the same range of temperature. If the first result was expected (similar variations of the viscosity are usually observed in nematics (*20*)), the second result is new and rather surprising.

2.5 *Summary of the main results in the thermal case*

From the previous experiments, it clearly appears that the Lehmann coefficient does not vanish at the compensation temperature at which the equilibrium twist vanishes. This is compatible with the symmetry of the phase at the compensation temperature which is different from that of a usual nematic (D_∞ instead of $D_{\infty h}$). As a consequence, the ansatz '$\nu \propto q$' proposed by theorists in the vicinity of T_c is incorrect. Another result is that the Lehmann coefficient increases (in absolute value) when the temperature increases, in contrast to the rotational viscosity which decreases. In addition, the Lehmann coefficient seems to strongly increase at the melting temperature, but further measurements are necessary to check this point definitely. Finally, note that we always implicitly assumed that the Lehmann coefficient was constant (for a given concentration of chiral molecules). This is not strictly correct as ν must also contain a term of the form $\xi(\boldsymbol{n} \cdot \nabla \times \boldsymbol{n} + q)$ which accounts for the helix deformation. Note that such a term (we could call this a 'nematic' term because it also exists in usual nematics, in which $q = 0$) was first introduced by Akopyan and Zel'dovich (*21*). Unfortunately, and in spite of the fact that the helix is deformed in most experiments, it was not yet possible to detect it (for a more complete discussion, see (*15*)). On the other hand, a similar term (associated to bend deformations) was measured in usual nematics by Akopyan *et al.* (*22*).

In the next section, we tackle the more difficult (and also controversial) problem of the electric Lehmann effect.

3. The electric Lehmann effect

As de Gennes pointed out in his book, an electric field should also produce a Lehmann torque:

$$\boldsymbol{\Gamma}_{\mathrm{Leh}} = -\nu_E \boldsymbol{E}_\perp, \tag{7}$$

where $\boldsymbol{E}_\perp = (\boldsymbol{n} \times \nabla) \times \boldsymbol{n}$ is the component of the electric field perpendicular to $\boldsymbol{n}$. The phenomenological coefficient ν_E is called, by extension, the electric Lehmann coefficient.

This effect was used in the past to interpret several experiments, but it seems today that in all of them, another explanation can be found for explaining the observed phenomena. In the following we briefly describe these experiments.

3.1 *First experimental evidence of rotating droplets under a DC electric field*

Performed in 1987 by Madhusudana and Prahtibha, this experiment was for a long time considered as the first direct proof of the existence of an electric Lehmann effect (*23*, *24*). In this experiment a cholesteric phase (mixture of two carboxylic esters with 5% cholesteryl choride) with a negative dielectric anisotropy is used. It is doped with a small quantity of epoxy resin (Lixon). This mixture, which exhibits a wide cholesteric–isotropic coexistence range at room temperature, is placed between two electrodes. Figure 12 shows an isolated droplet suspended in the isotropic liquid rotating clockwise under a positive DC voltage and anticlockwise under a negative DC voltage. In this experiment, the cholesteric helix is almost everywhere oriented perpendicularly to the glass plates. Note that the applied voltage favours this orientation as the liquid crystal has a negative dielectric anisotropy. A κ disclination line of rank two is visible on the curved side of the droplet. This defect is imposed by the planar anchoring condition at the cholesteric–isotropic interface (for a description of the director field topology, see (*25*)). One important point in this experiment is that there is a thin layer of isotropic liquid rich in Lixon between the droplet and the electrodes which plays exactly the same role as the sliding planar anchoring used in our own experiments

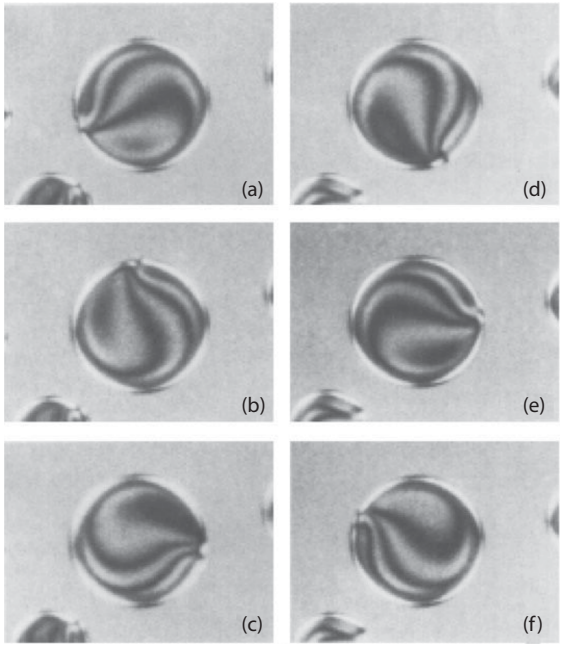

Figure 12. Droplet turning: (a),(b),(c) clockwise under a +2 V DC voltage; and (d),(e),(f) anticlockwise under a –2 V DC voltage (reproduced with permission from (*23*)).

(see Sections 2.2 and 2.4). In this way, the droplets (more exactly their internal texture) can turn freely. In addition, Madhusudana and Pratibha observed that the rotation velocity of the droplet does not depend on their size, changes sign when the chiral impurity methyl butyl benzoyloxy heptyloxy cinnamate is used instead of CC, and is linear in the applied voltage provided it is large enough (screening effects occur at voltages less than 1.8 V).

For all of these reasons, Madhusudana and Pratibha interpreted their experiment in terms of electric Lehmann effect. Doing this they found that the electric Lehmann coefficient was proportional to q with

$$|\frac{\nu_E}{q}| \approx 0.6 \times 10^{-12}\,\mathrm{C\,m^{-1}}.$$

Here the linear dependence between ν_E and q is not surprising because these two quantities are linear in C, the concentration of chiral impurities, provided that C is small enough ($\nu_E = 0$ and $q = 0$ at $C = 0$).

It is worth noting that the droplets of Madhusudana and Pratibha are different from ours and those of Lehmann (compare Figures 2, 11 and 12). Another difference is that our droplets slow down when their diameter D increases whereas the droplets of Madhusudana and Pratibha rotate at constant velocity whatever their diameter. This result can be explained in terms of texture. Indeed, in the banded droplets, the dissipation increases as D^4k^2 (see (*19*)), whereas in the droplets of Madhusudana and Pratibha, where the texture is homogeneous except on the side, this quantity increases as D^2 (see (*24*)). As the Lehmann torque integrated over a whole droplet increases as D^2 in both cases, it comes out that the banded droplets slow down when their diameter increases, whereas the Madhusudana and Pratibha droplets rotate at constant speed whatever their size.

This interpretation was recently questioned by Tarasov (*26*). He proposed to explain the experiment of Madhusudana and Pratibha by only using the classical electrohydrodynamic model without introducing the electric Lehmann effect. More precisely he showed by using an approximate model for the director field inside the droplets (*25*), that the charge generation due to flexoelectric polarization can explain the droplet rotation with properties similar to those found in the experiment.

At this level, it is difficult to discriminate between the two models. On the other hand, the two experiments presented in the next two Sections strongly suggest that Tarasov is right.

3.2 Electrically driven drift of CF in homeotropic samples

It has been well known for a long time that CF (see Figure 8) can drift and form spirals similar to those shown in Figures 9 and 10 under the action of a DC or an AC electric field (for a review see (*9*) or (*10*)). We recall that spirals under AC electric field were first observed by Gilli and Kamayé (*27*) and Mitov and Sixou (*28*) in a polymeric cholesteric mixture and then by Ribiére *et al.* (*29*) in usual cholesterics. As for spirals formed under DC electric field, they were first observed by Hinov and Klukeva (*30*) and then studied in more details by Gil *et al.* (*31, 32*).

In practice all CF drift under a DC electric field. By contrast, and for symmetry reasons as can be seen by comparing the two types of fingers (see Figure 13), only CF of the second type (CF2) (*33, 34*) can drift in an AC electric field. The reason is that for CF2 the drift velocity is different (in absolute value) when the electric field points upwards or downwards, resulting in a non-zero velocity under AC electric field. By contrast, the drift velocity of a CF1 reverses, but does not change amplitude, when the field reverses, so that it cannot drift in average in an AC electric field.

It is obvious that the electric Lehmann effect is a good candidate to explain the finger drift as was shown first by Gil and Thiberge (*17*) (we recall that we used a similar model in Section 2.3 to explain the drift of CF1 in a thermal gradient (*18*)). This model was then extended to CF2 by Gil and Gilli (*33*) to

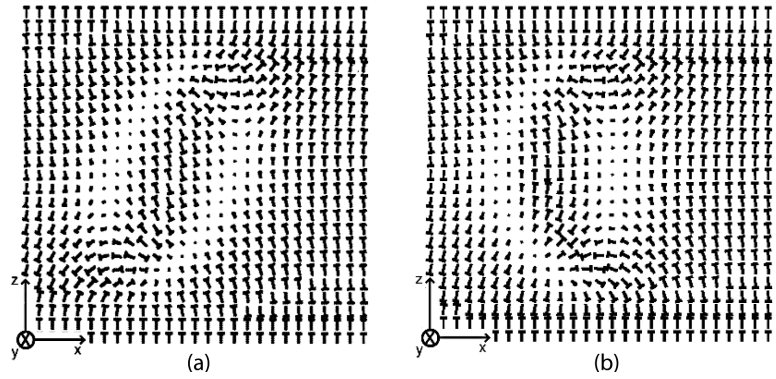

Figure 13. Nail representation of (a) a CF1 and (b) a CF2. Owing to the $\boldsymbol{n} \rightarrow -\boldsymbol{n}$ invariance, a CF1 is unchanged by a π rotation around the y-axis. Suppose that the finger drifts with a velocity $-\boldsymbol{V} \parallel \boldsymbol{x}$ under the action of the electric field $\boldsymbol{E} \parallel \boldsymbol{z}$. Applying a π rotation around the y-axis, we find that the same finger drifts with velocity $-\boldsymbol{V}$ under the action of the electric field $-\boldsymbol{E}$. This is the reason why a CF1 does not drift in average under AC electric field. By contrast, a CF2 is not invariant by a π rotation. This symmetry breaking explains why a CF2 may drift under AC electric field (reproduced with permission from (*33*)).

explain their drift under AC field. These authors found that the drift velocity of CF2 exponentially decreases with the frequency of the applied voltage. A quite similar behaviour was also found in the presence of flexoelectricity.

To test these different hypotheses, Baudry *et al.* (*35*) systematically measured the drift velocity of CF2 in samples of various thicknesses and conductivities (by adding ionic impurities) (Figure 14). They found, among other properties, that

(1) the CF2 stop drifting when the frequency of the applied electric field becomes larger than the charge relaxation frequency of the sample ($f > f_{\text{relax}}$);
(2) the CF2 drift velocity is independent of the conductivity (and, thus, of the concentration of ionic impurities) at low frequency ($f < f_{\text{relax}}$).

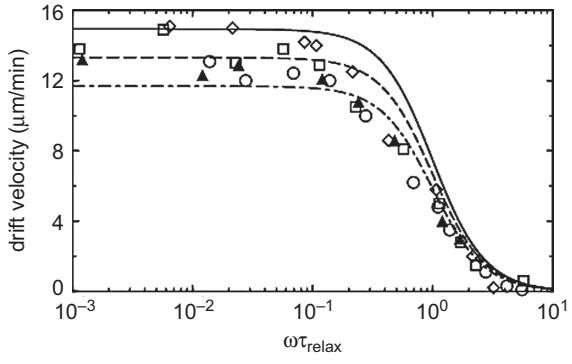

Figure 14. Drift velocity of CF2 versus reduced frequency of the AC electric field. Points are experimental data from (*35*) and lines are calculations performed from the standard electrohydrodynamic model for different values (1.3, 1.4 and 1.5 from top to bottom) of the ratio of the electric conductivities $\sigma_{\parallel}/\sigma_{\perp}$ (reproduced with permission from (*36*)).

These two properties are hardly compatible with the model of Gil *et al.* For this reason, Tarasov *et al.* (*26, 36*) proposed to reanalyse this problem in the framework of the usual electrohydrodynamic model. They found that electrohydrodynamic effects induced by the classical Carr–Helfrich charge separation mechanism (*5, 9*) can reproduce quite well the experimental data.

The same authors also interpret the experiments of Gil and Thiberge about the drift of CF1 under DC electric field by introducing electrohydrodynamic effects induced by flexoelectric charge separation (we recall they also explained the drop rotation observed by Madhusudana and Pratibha in the same way).

As a consequence, it does not seem necessary to include an electric Lehmann effect to explain the finger drift or the droplet rotation under electric field. This does not mean that the electric Lehmann effect does not exist (it is not forbidden by symmetries), but just that it is certainly masked by other phenomena quantitatively more important.

The experiment described in the next section reinforces this conclusion.

3.3 The Padmini and Madhusudana experiment

In 1991, Madhusudana *et al.* (*37*) proposed a new experiment to provide evidence of the Lehmann electromechanical effect in cholesterics of positive dielectric anisotropy. The experiment was as follows: the liquid crystal was confined between two parallel electrodes treated for strong planar and parallel anchoring. The sample thickness d was chosen to be slightly less than $p/4$ (Figure 1) in order that the cholesteric was unwound. The sample was illuminated with a He–Ne laser beam at normal incidence and

was subjected to an AC electric field $E = V/d$ of frequency f. The experiment consisted of analysing with a lock-in amplifier the f component I_1 (first harmonic) of the transmitted intensity $I(t)$ between crossed polarizer and analyser, with the polarizer making an angle of $\pi/8$ with the anchoring direction to obtain the maximal signal intensity. These authors found that $|I_1|$ was not measurable at small voltage whereas its modulus became measurable above the onset of the Freedericksz instability ($V > V_c$). This signal was interpreted as a direct manifestation of the Lehmann thermomechanical coupling.

The same authors observed a similar response in a non-chiral nematic phase twisted by 20° above the onset of the Freedericksz instability, concluding that an electromechanical coupling also exists in a distorted nematic (*37*).

Fortified by these results, Padmini and Madhusudana (*38*) generalized the previous experiment to a compensated cholesteric mixture. They again found that the first harmonic of the signal was only measurable above the onset of the Freedericksz instability. However, the new result was that the first harmonic vanishes and changes sign at the inversion temperature T_c. From this observation, Padmini and Madhusudana concluded that the electric Lehmann coefficient was equal to zero at T_c and proportional to q close to T_c, as proposed by theorists.

It appears that these results clearly disagree with the previous experiments performed in the thermal case on a compensated cholesteric. For this reason, we repeated the Padmini and Madhusudana experiment and looked for another explanation for the observed phenomena.

In our experiments, we again used the 8OCB-CC mixture in mass proportion 1:1. Samples with strong parallel planar anchoring were prepared between two transparent electrodes. Sample thickness was 5 μm. We first measured the two components X_1 and Y_1 of the first harmonic as a function of temperature around T_c. By definition, $X_1 = |I_1| \cos \Phi$ and $Y_1 = |I_1| \sin \Phi$ where Φ is the phase shift of I_1 with respect to the sinusoidal applied voltage $V = V_0 \sin(2\pi ft)$. Figure 15 shows the signal as a function of applied voltage when the helix is unwound ($d < p/4$) while Figure 16 shows the signal measured above the threshold as a function of temperature. In agreement with Padmini and Madhusudana, we observed that:

(1) there is no signal below V_c;
(2) the signal is almost in quadrature with the voltage above V_c ($|X_1| \ll |Y_1|$) and decreases as $1/f$;
(3) the signal vanishes and changes sign at the compensation temperature.

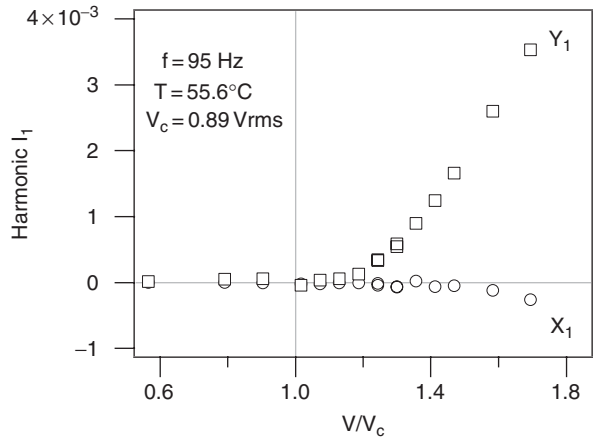

Figure 15. Harmonic 1 as a function of the relative shift to the critical voltage. Note that the signal was normalized to the intensity I_0 measured below V_c (reproduced with permission from (*57*)).

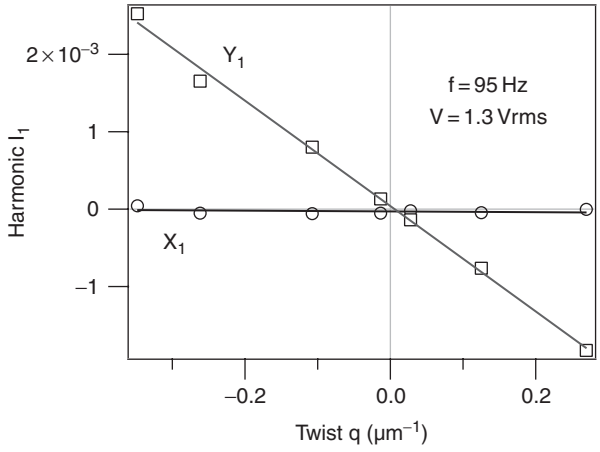

Figure 16. Normalized harmonic 1 as a function of the spontaneous twist (reproduced with permission from (*57*)).

In complement, we performed the same experiment when the director field was twisted through 180° within the sample thickness. In this case, the temperature was chosen in order that $d = p/2$. We again observed the absence of a measurable signal below V_c and a strong signal above V_c.

We then reanalysed all of these data in terms of Lehmann and flexoelectric effects. Indeed, it has been well known for a long time that flexoelectricity exists in cholesterics (*39*) and most often couples with the Lehmann thermomechanical effect (*40*). For this reason, we solved semi-analytically the director field close to the onset of instability and calculated the corresponding transmitted intensity (for more details see (*41–42*)) in the two limiting cases: $v_E \neq 0$ with $e_3 - e_1 = 0$ and $v_E = 0$ with $e_3 - e_1 \neq 0$. Here e_1 (respectively, e_3) is the flexoelectric coefficient related to

bend (respectively, splay) distortion (*5*, *9*). Note that in the case $v_E \neq 0$, we did two different assumptions, namely $v_E \propto q$ and $v_E \propto \boldsymbol{n} \cdot \nabla \times \boldsymbol{n}$. Our conclusion was that the experimental results are incompatible with an electric Lehmann effect, whereas the flexoelectricity allows one to reproduce pretty well the whole data set in both unwound and twisted geometries.

3.4 Summary of the main results in the electric case

From all of these experiments, it emerges that the electric Lehmann effect predicted by de Gennes is difficult to measure because it is often masked by other phenomena such as flexoelectricity under AC electric field or the Carr–Helfrich phenomenon under DC field. In particular, the value given by the Bangalore group for v_E is probably not realistic.

In the next section, we report recent experiments about the chemical Lehmann effect.

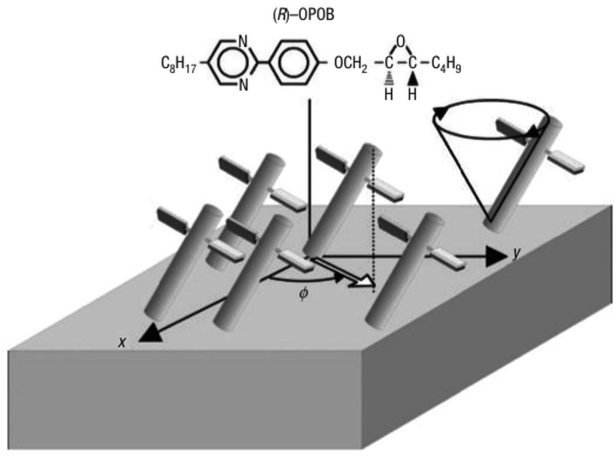

Figure 17. The chemical structure of (R)-OPOB and a schematic representation of its Langmuir monolayer spread on glycerol. The pair of small wings attached to the molecules represent the chiral group which acts as a propeller. The angle Φ gives the orientation of the director. Reprinted by permission from Macmillan Publishers Ltd (*43*), Copyright © (2003).

4. The chemical Lehmann effect

As we recalled in the introduction, a gradient of chemical potential should also produce a Lehmann torque.

This was first emphasized by de Gennes in his book, but it is only very recently that this effect has been clearly observed by Tabe and Yokoyama in a Langmuir monolayer (*43*) (see also the recent experiments of Milczarczyk-Piwowarczyk *et al.* (*44*) and Gupta *et al.* (*45*)). In the Tabe and Yokoyama experiment, a monolayer of the chiral rod-like molecules (R)-OPOB is deposited on the free surface of a glycerol–water mixture. As these molecules tilt from the surface normal, they form a two-dimensional ferronematic phase (Figure 17).

Observations using reflected-light microscopy reveal that soon after the film has been formed, concentric rings grow inside the initially well-orientated domains provided that the pressure difference $\Delta P_w = P_v - P_s$ is not zero (Figure 18). Here P_v is the actual vapor water pressure and P_s is the saturated vapor water pressure on the given glycerol–water mixture. This reveals a continuous rotation of the director which is driven by the flux of water molecules across the monolayer. Careful observations show that the angular frequency is proportional to ΔP_w (linear effect). Finally, the angular frequency changes sign when the other enantiomer (S)-OPOB is used.

All of these observations clearly reveal a chemical Lehmann effect. This discovery led to several theoretical papers analysing the pattern formation in these films, those (including de Gennes) focusing on the role of defects (*46*) or noise (*47*), while others tackle more complex phenomena such as the coupling between the local concentration and the director field distortion (*48, 49*). We mention also a recent theoretical work about the inverse chemical Lehmann effect which could be used as a microscopic pump (*50*). Finally, note that the direct and inverse chemical Lehmann effect should also exist in free films of smectic C* as was already mentioned a long time ago by Brand and Pleiner (*51*). These two effects were recently observed by Blanc *et al.* (*52*) in Montpellier and by Tabe in Tokyo (*53*), but their results are not yet published (to the best of our knowledge).

5. Concluding remarks

It seems today that both the thermal and chemical Lehmann effects are well established, by contrast with the electric Lehmann effect.

In the thermal case, we emphasize that all experiments, except those of Lehmann, were performed with compensated cholesteric mixtures which are all very rich in chiral molecules. Nevertheless, recent experiments performed with more classical mixtures of cyanobiphenyls doped with small amounts of the chiral agent S811 (from Merck) show similar behaviour, even at concentrations as small as 0.5% by weight. These results (*54*) are compatible with Lehmann's observations. One very interesting point concerns the value of the Lehmann coefficient. Indeed, we have found that $v \approx 10^{-7}$ kg K^{-1} s^{-2} at the compensation temperature which gives a torque per unit volume vG of the order of 10^{-2} J m^{-3} by taking the larger temperature gradient used in experiments

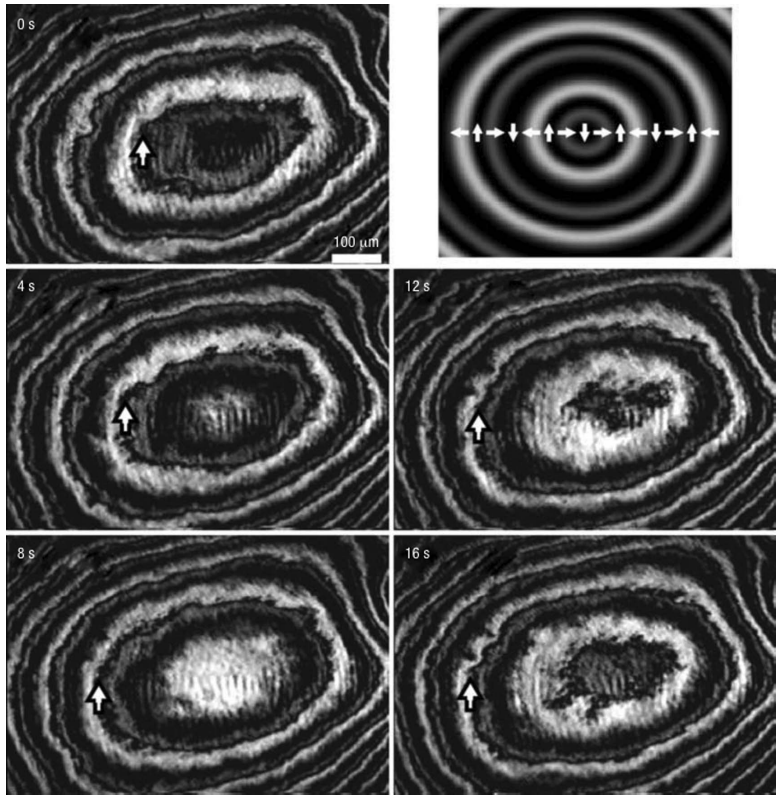

Figure 18. Sequence of micrographs showing the rotation of the director under the action of a flux of water molecules. The director field organization is shown in the top right inset. Reprinted by permission from Macmillan Publishers Ltd (*43*), Copyright © (2003).

($G \sim 10^5$ K m^{-1}). This gives a torque per chiral molecule of the order of $3 \times 10^{-9}\ k_BT$, thus much smaller than the thermal energy. This indicates that a high degree of self-organisation is needed to overcome the thermal fluctuations. This is indeed the case in a cholesteric phase where the orientational order (characterized by the quadrupolar order parameter Q first introduced by de Gennes (*5*)) is long range. On the other hand, all experiments seem to indicate that the Lehmann coefficient increases with temperature with a maximum at the melting temperature. This result is counterintuitive because the order parameter Q characterizing the degree of self-organization rapidly decreases at the transition. At this level one could speculate that v is proportional to dQ/dT, but this assumption remains to be proven. Another explanation could be that other mechanisms occur in droplets or fingers, as they involve complicated director fields. This hypothesis was raised by Tarasov *et al*. (*36*) who proposed to use a new 'thermohydrodynamic' approach to explain the droplet rotation and the finger drift in a thermal gradient (in analogy with what they did in the case of fingers or droplets subjected to an electric field). However, it is still too early to conclude about the relevance of such a model as no calculation has been performed in this direction so far. Finally, note that Sarman performed non-equilibrium molecular dynamic simulations of the thermal Lehmann effect and observed the helix rotation (*55–57*). On the other hand, the value of v he found numerically is typically four or five orders of magnitude larger than that measured experimentally in the compensated mixtures. This certainly comes from the crudeness of the model in which, for instance, only steric interactions between molecules are taken into account.

The situation is still more complex in the case of the electric Lehmann effect. The reason is that for the moment, all of the proposed experiments involve (at least at large field) other mechanisms (such as the flexoelectricity or the Carr–Helfrich mechanism, for instance) which dominate the expected electric Lehmann effect. It is nevertheless a bit surprising that the latter was not detected in the Padmini and Madhusudana geometry under the onset of Freedericksz instability. This could be due to the too small value of the imposed electric field. In the future, it would be interesting to perform a similar experiment using a compensated mixture with a negative dielectric anisotropy in order to avoid the Freedericksz instability

at high voltage. This should allow one to use a larger field on condition, however, of not exceeding the onset of electrohydrodynamic convection.

Last but not least, the chemical Lehmann effect predicted by de Gennes has been discovered recently in chiral ferronematic Langmuir monolayers and in SmC* free films. This discovery confirms once again the genial intuition of de Gennes. It is important in itself and for applications as it open the possibility to realize molecular pumps. Also interesting is the value of the torque per molecule that the 'flowing' molecules (water in experiments) exert on the chiral molecules. According to Tabe and Yokoyama (*42*), this torque is of the order of 10^{-10}–10^{-11} k_BT. This value is again very small (and even smaller than in the thermal case) and confirms the importance of the collective effects in this problem.

In the longer term, we hope that this short (and non-exhaustive) review will stimulate further experiments and will encourage theorists to work on this fascinating effect and its microscopic origin.

References

(1) Lehmann, O. *Ann. Phys.* **1900**, *307*, 649–705.
(2) Friedel, G. *Ann. Phys.* E **1922**, *18*, 273–474.
(3) Lehmann, O. *Flüssige Krystalle und ihr scheinbares Leben*; Verlag von Leopold Voss: Leipzig, 1921.
(4) Leslie, F.M. *Proc. R. Soc. A* **1968**, *307*, 359–372.
(5) de Gennes, P.-G. *The Physics of Liquid Crystals*; Oxford: Clarendon Press, 1974.
(6) Éber, N.; Jánossy, I. *Mol. Cryst. Liq. Cryst. Lett.* **1982**, *72*, 233–238.
(7) Éber, N.; Jánossy, I. *Mol. Cryst. Liq. Cryst. Lett.* **1984**, *102*, 311–316.
(8) Éber, N.; Jánossy, I. *Mol. Cryst. Liq. Cryst. Lett.* **1988**, *5*, 81–86.
(9) Oswald, P.; Pieranski, P. *Nematic and Cholesteric Liquid Crystals: Concepts and Physical Properties Illustrated by Experiments*; Taylor and Francis/CRC Press: London, 2005.
(10) Oswald, P.; Baudry, J.; Pirkl, S. *Phys. Rep.* **2000**, *337*, 67–96.
(11) Pleiner, H.; Brand, H.R. *Mol. Cryst. Liq. Cryst. Lett.* **1987**, *5*, 61–65.
(12) Pleiner, H.; Brand, H.R. *Mol. Cryst. Liq. Cryst. Lett.* **1988**, *5*, 183–186.
(13) Dequidt, A.; Oswald, P. *Europhys. Lett.* **2007**, *80*, 26001 p1–5.
(14) Dequidt, A.; Żywociński, A.; Oswald, P. *Eur. Phys. J. E* **2008**, *25*, 277–289.
(15) Oswald, P.; Dequidt, A. *Europhys. Lett.* **2008**, *83*, 16005 p1–5.
(16) Oswald, P.; Dequidt, A.; Żywociński, A. *Phys. Rev. E* **2008**, *77*, 061703 p1–9.
(17) Gil, L.; Thiberge, S. *J. Phys. II* **1997**, *7*, 1499–1508.
(18) Oswald, P.; Dequidt, A. *Phys. Rev. E* **2008**, *77*, 051706 p1–5.
(19) Oswald, P.; Dequidt, A. *Phys. Rev. Lett.* **2008**, *100*, 217802 p1–4.
(20) Kneppe, H.; Schneider, F.; Sharma, N.K. *J. Chem. Phys.* **1982**, *77*, 3203–3208.
(21) Akopyan, R.S.; Zel'dovich, B.Ya. *Sov. Phys.–JETP* **1984**, *60*, 953–960.
(22) Akopyan, R.S.; Alaverdian, R.B.; Santrosian, E.A.; Chilingarian, Y.S. *J. Appl. Phys.* **2001**, *90*, 3371–3376.
(23) Madhusudana, N.V.; Pratibha, N. *Mol. Cryst. Liq. Cryst. Lett.* **1987**, *5*, 43–51.
(24) Madhusudana, N.V.; Pratibha, N. *Liq. Cryst.* **1989**, *5*, 1827–1840.
(25) Bajc, J.; Žumer, 1997, *Phys. Rev. E*, **55**, 2925–3937.
(26) Tarasov, O.S. Structural Transitions and Dynamics of Liquid Crystals under Flows and Electric Fields; Ph.D. Thesis, University of Bayreuth, 2003.
(27) Gilli, J.M.; Kamayé, M. *Liq. Cryst.* **1992**, *11*, 791–796.
(28) Mitov, M.; Sixou, P. *J. Phys. II* **1992**, *2*, 1659–1670.
(29) Ribiére, P.; Oswald, P.; Pirkl, S. *J. Phys. II* **1994**, *4*, 127–143.
(30) Hinov, H.P.; Kukleva, E. *Mol. Cryst. Liq. Cryst.* **1984**, *109*, 203–224.
(31) Frisch, T.; Gil, L.; Gilli, J.M. *Phys. Rev. E* **1993**, *48*, R4199–R4202.
(32) Gilli, J.M.; Gil, L. *Liq. Cryst.* **1994**, *17*, 1–15.
(33) Gil, L.; Gilli, J.M. *Phys. Rev. Lett.* **1998**, *80*, 5742–5745.
(34) Baudry, J.; Pirkl, S.; Oswald, P. *Phys. Rev. E* **1999**, *59*, 5562–5571.
(35) Baudry, J.; Pirkl, S.; Oswald, P. *Phys. Rev. E* **1999**, *60*, 2990–2993.
(36) Tarasov, O.S.; Krekhov, A.P.; Kramer, L. *Phys. Rev. E* **2003**, *68*, 031708 p1–4.
(37) Madhusudana, N.V.; Pratibha, N.; Padmini, H.P. *Mol. Cryst. Liq. Cryst.* **1991**, *202*, 35–49.
(38) Padmini, H.P.; Madhusudana, N.V. *Liq. Cryst.* **1993**, *14*, 497–511.
(39) Patel, J.S.; Meyer, R.B. *Phys. Rev. Lett.* **1987**, *58*, 1538–1541.
(40) Brand, H.R.; Pleiner, H. *Mol. Cryst. Liq. Cryst.* **1997**, *292*, 141–146.
(41) Dequidt, A.; Oswald, P. *Eur. Phys. J. E* **2007**, *24*, 157–166.
(42) Dequidt, A. Effet Lehmann dans les cristaux liquides cholestériques; Ph.D. Thesis, Université de Lyon, Ecole Normale Supérieure de Lyon, 2008.
(43) Tabe, Y.; Yokoyama, H. *Nature Mater.* **2003**, *2*, 806–809.
(44) Milczarczyk-Piwowarczyk, P.; Żywociński, A.; Noworyta, K.; Holyst, R. *Langmuir* **2008**, *24*, 12354–12363.
(45) Gupta, R.K.; Suresh, K.A.; Kumar, S.; Lopatina, L.M.; Selinger, R.L.B.; Selinger, J.V. *Phys. Rev. E* **2008**, *78*, 041703 p1–7.
(46) Tsori, Y.; de Gennes, P.-G. *Eur. Phys. J. E* **2004**, *14*, 91–96.
(47) Svenšek, D.; Pleiner, H.; Brand, H.R. *Phys. Rev. Lett.* **2006**, *96*, 140601–4.
(48) Shibata, T.; Mikhailov, A.S. *Europhys. Lett.* **2006**, *73*, 436–442.
(49) Shibata, T.; Mikhailov, A.S. *Chaos* **2006**, *16*, 037108 p1–8.
(50) Svenšek, D.; Pleiner, H.; Brand, H.R. *Phys. Rev. E* **2008**, *78*, 021703 p1–4.
(51) Brand, H.R.; Pleiner, H. *Phys. Rev. A* **1988**, *37*, 2736–2738.
(52) Blanc, C.; Goc, F.; Nobili, M.; Lorman, V.L. Poster at the *21st International Liquid Crystal Conference*, Keysone, Colorado, 2006.

(53) Tabe, Y. Invited talk IL8 at the *European Conference on Liquid Crystals*, ECLC abstract CDROM, issued by Universidade Nova de Lisboa, Faculdade de Ciências e Tecnologia, 2007, p. 58.
(54) Oswald, P. Lehmann rotation of cholesteric droplets subjected to a temperature gradient: role of the concentration of chiral molecules, accepted to *Eur. Phys. J. E*, **2009**, *28*, 377–383.
(55) Sarman, S. *J. Chem. Phys.* **1999**, *110*, 12218–12225.
(56) Sarman, S. *Mol. Phys.* **2001**, *98*, 27–35.
(57) Sarman, S. *Mol. Phys.* **2001**, *99*, 1235–1247.